Sources of black carbon aerosols in South Asia and surrounding regions during the Integrated Campaign for Aerosols, Gases and Radiation Budget (ICARB)

Rajesh Kumar[1,2], M. C. Barth[2], Vijayakumar S. Nair[3], G. G. Pfister[2], S. Suresh Babu[3], S. K. Satheesh[4], K. Krishna Moorthy[5], G. R. Carmichael[6], Z. Lu[7], D. G. Streets[7]

[1]Advanced Study Program, National Center for Atmospheric Research, Boulder, USA

[2]Atmospheric Chemistry Division, National Center for Atmospheric Research, Boulder, USA

[3]Space Physical Laboratory, Vikram Sarabhai Space Center, Thiruvanantpuram, India

[4]Centre for Atmospheric and Oceanic Sciences, Indian Institute of Science, Bangalore, India

[5]Indian Space Research Organization (Hq), New BEL Road, Bangalore, India

[6]Center for Global and Regional Environmental Research, University of Iowa, Iowa City, IA 52242, USA

[7]Energy Systems Division, Argonne National Laboratory, Argonne, IL 60439, USA

Correspondence to: Rajesh Kumar (rkumar@ucar.edu)

Running title: Sources of BC aerosols in South Asia during ICARB

Abstract

This study examines differences in the surface black carbon (BC) aerosol loading between the Bay of Bengal (BoB) and the Arabian Sea (AS), and identifies dominant sources of BC in South Asia and surrounding regions during March-May 2006 (Integrated Campaign for Aerosols, Gases and Radiation Budget, ICARB) period. A total of 13 BC tracers are introduced in the Weather Research and Forecasting Model coupled with Chemistry to address these objectives. The model reproduced the temporal and spatial variability of BC distribution observed over the AS and the BoB during the ICARB ship-cruise, and captured spatial variability at the inland sites. In general, the model underestimates the observed BC mass concentrations. However, the model-observation discrepancy in this study is smaller compared to previous studies. Model results show that ICARB measurements were fairly well representative of the Arabian Sea and the Bay of Bengal during the pre-monsoon season. Elevated BC mass concentrations in the BoB are due to five times stronger influence of anthropogenic emissions on the BoB compared to the AS. Biomass burning in Burma also affects the BoB much more strongly than the AS. Results show that anthropogenic and biomass burning emissions, respectively, accounted for 60% and 37% of the average ± standard deviation (representing spatial and temporal variability) BC mass concentration (1341±2353 ng m^{-3}) in South Asia. BC emissions from residential (61%) and industrial (23%) sectors are the major anthropogenic sources, except in the Himalayas where vehicular emissions dominate. We find that regional-scale transport of anthropogenic emissions contributes up to 25% of BC mass concentrations in western and eastern India, suggesting that surface BC mass concentrations cannot be linked directly to the local emissions in different regions of South Asia.

1. Introduction

Black carbon (BC), a byproduct of incomplete combustion, is a key atmospheric aerosol species because it contributes largely to the climate forcing (e.g. Ramanathan and Carmichael, 2008; Wang et al., 2014; Hodnebrog et al., 2014) and, along with other fine particulates, adversely affects human health (e.g. Dockery and Stone, 2007). BC is emitted from various sources including industries, motor vehicles, power plants, residential solid biofuel burning, and open biomass burning of forests, savannas and crop residues. The total global emissions of BC aerosol estimated using bottom-up approaches are 7500 Gg $year^{-1}$ in the year 2000 with an uncertainty range of 2000 to 29000 Gg $year^{-1}$ (Bond et al., 2013). BC has very low chemical reactivity in the atmosphere and is removed primarily by the wet and dry depositions at the surface. However, the wet deposition represents 70-85% of the global total loss (Pöschl, 2005). The average atmospheric lifetime of BC is estimated to be about a week (Bond et al., 2013) enabling BC aerosols to undergo regional and intercontinental transport.

Different emission sources of BC show strong regional variations (Lawrence and Lelieveld, 2010; Lu et al., 2011; Bond et al., 2013) and South Asia with its large population density involved in a wide range of human activities is considered to be one of the hotspots of BC emissions (Bond et al., 2007). In addition, different emission inventories show an increasing trend in BC emissions over South Asia (Granier et al., 2011). Large emissions of BC in South Asia lead to BC-induced radiative perturbation which is significantly higher than the globally averaged estimates (Babu et al., 2004; Ramanathan and Carmichael, 2008). Model estimates show that this forcing has the potential to affect the Asian Summer Monsoon (Ramanathan et al., 2005; Lau et al., 2006) and Himalayan glaciers (e.g. Menon et al., 2010; Yasunari et al., 2010).

Many efforts have been made to measure BC mass concentration, document its diurnal, seasonal and spectral (absorption) characteristics and estimate local scale BC-induced radiative perturbation in a wide range of atmospheric conditions (urban, rural, marine and high altitude mountains) in South Asia (e.g. Satheesh and Ramanathan, 2000; Babu et al., 2004; Beegum et al., 2009; Gustafsson et al., 2009; Nair et al., 2008, 2013; Marrapu et al., 2014). The regional and global scale radiative impacts of BC and other short-lived pollutants emitted from different sectors have also been estimated in some global modeling studies (e.g. Reddy et al., 2005; Unger et al., 2009, 2010; Verma et al., 2011). However, the relative contributions of different emission sources to atmospheric BC mass concentrations are still unknown for South Asia except for the Delhi region, where the majority of the atmospheric BC is attributed to emissions from transportation (~59%) and domestic (~32%) sectors (Marrapu et al., 2014).

Chemical transport models serve as our primary tool for establishing the relation between the amount of a species emitted and its atmospheric concentration. However, a detailed evaluation of such models is required before conducting such an analysis. In this study, we first evaluate the performance of the Weather Research and Forecasting Model (Skamarock et al., 2008) coupled with Chemistry (WRF-Chem) (Grell et al., 2005; Fast et al., 2006) using high resolution BC measurements made as a part of the Integrated Campaign for Aerosols, Gases and Radiation Budget (ICARB) (Moorthy et al., 2008). The evaluation exercise also provides confidence in using the model for future studies. The evaluated WRF-Chem configuration is then used to answer the following two questions: (a) why is aerosol loading higher over the Bay of Bengal compared to the Arabian Sea? and (b) what were the most important sources of surface BC

aerosols in South Asia during the ICARB? It is important to answer the first question because the stronger aerosol radiative forcing over the Bay of Bengal has been suggested to affect the monsoonal circulation and rainfall over South Asia (Bollasina et al., 2013). The answer to the second question has implications for improving air quality in South Asia but we need to extend this analysis to multiple years to account for long-terms changes in the aerosol emissions and meteorology. This study focuses only on the ICARB period. Source contribution analysis for a complete year is discussed in a separate paper (Kumar et al., 2015). To answer the above questions, we introduce source, sector and region specific BC tracers in WRF-Chem.

We begin with a description of ICARB observations, WRF-Chem configuration and implementation of BC tracers in the WRF-Chem. In the Results section, we first evaluate the model performance and then quantify the contribution of different emission sources and sectors to total BC loading and demonstrate the importance of regional transport in distribution of BC in the atmosphere of South Asia.

2. Experimental Design

We use version 3.5.1 of the WRF-Chem model to simulate the geographical distribution of BC in South Asia and surrounding regions. Recently, we set-up WRF-Chem over South Asia and demonstrated that WRF-Chem is able to capture observed variations in meteorology (Kumar et al., 2012a), gas-phase chemistry (Kumar et al., 2012b; 2013) and dust aerosols (Kumar et al., 2014a, 2014b) over South Asia. However, the model's ability to simulate BC in South Asia and surrounding regions has not been tested so far. In this study, we attempt to fill this gap by comparing WRF-Chem simulated BC with extensive measurements of BC made over the Bay of

Bengal (BoB) and the Arabian Sea (AS) during 18 March-11 May 2006 during ICARB (see Figure 1 for ship-track) (Moorthy et al., 2008), and average BC values reported at 12 inland stations in the model domain. ICARB was an integrated multi-instrument, multi-platform field campaign and provided extensive co-located measurements of several aerosol parameters and trace gases over the Bay of Bengal, northern Indian Ocean and the Arabian Sea. ICARB observations revealed large spatio-temporal heterogeneities in several aerosol parameters including the BC mass concentrations and trace gases over the oceanic regions around India (Moorthy et al., 2008; Nair et al., 2008; Srivastava et al., 2012).

During the ocean segment of ICARB, a special laboratory was configured at the top deck of the ship called "Sagar Kanya" and ambient air was drawn from a height of about 10 m above the water level into various instruments deployed for measurements of trace gases and aerosols. BC mass concentrations were measured using an Aethalometer (AE 21 of Magee Scientific) operated at a time base of 5 min and flow rate of 5 L per minute. The ship sailed in the BoB and the northern Indian Ocean during 9 March to 13 April 2006 and during 18 April to 11 May in the AS. The meteorological conditions prevailing during the ICARB were composed mainly of calm synoptic conditions with weak winds, clear skies and absence of precipitation (except for 9 April). The ship did not face any major weather system or cyclonic depression during the whole campaign. Analysis of synoptic scale wind patterns showed the presence of weak westerly winds in the northern BoB associated with a low-level anticyclonic circulation centered at (88^{o}E, 15^{o}N), and weak easterly winds prevailed south of 12^{o}N in the BoB. During the AS segment of the campaign, the synoptic winds were strong westerlies in the northern AS, which turned sharply to northerlies close to the peninsular India due to presence of a strong anticyclone at

132 (60^{o}E, 16^{o}N). Further details of the ship-cruise track, measurement set-up, uncertainties, quality
133 control and analysis of BC measurements, and meteorological conditions during ICARB are
134 discussed in Nair et al. (2008).
135
136 In addition, we use average BC values reported for March to May at 12 stations in the model
137 domain (Table 1). These stations are located in a wide range of chemical environments with
138 Delhi, Kanpur, Kharagpur and Dibrugarh representing urban/semi-urban sites, Lhasa
139 representing a high altitude urban site, Trivandrum representing a coastal semi-urban site,
140 Nainital, Nagarkot, Langtang and Nepal Climate Observatory – Pyramid (NCO-P) representing
141 high altitude cleaner sites, and Minicoy and Port-Blair representing island sites, respectively.
142
143 The WRF-Chem domain covers South Asia and surrounding oceanic regions with a horizontal
144 grid spacing of 36 km (Figure 1) and 35 levels from surface to 10 hPa. Aerosol processes are
145 represented by the Model for Simulating Aerosol Interactions and Chemistry (MOSAIC, Zaveri
146 et al., (2008)) using 4 size bins. MOSAIC treats black carbon as internally mixed with other
147 major aerosol species including sulfate, nitrate, organic carbon, liquid water, methanesulfonate,
148 chloride, carbonate, ammonium, sodium, calcium, and other inorganics (including dust) within
149 each size bin. The aerosol particles are considered as hydrophilic and can activate to form cloud
150 droplets. Aerosol particles are subjected to both dry and wet deposition (in- and below- cloud
151 scavenging) where the dry deposition module follows Binkowski and Shankar (1995) and wet
152 deposition module follows Easter et al. (2004). Wet deposition represents the major loss (~84%)
153 process for BC in our model domain. The gas-phase chemistry is represented by Model for
154 Ozone and Related Tracers (MOZART) chemical mechanism (Emmons et al., 2010; Knote et al.,

2014). Initial and lateral boundary conditions for meteorological and chemical fields are obtained from 6-hourly NCEP Final Analysis Fields and MOZART-4 results (Emmons et al., 2010) respectively. Analysis nudging is applied to horizontal winds, moisture and temperature above the planetary boundary layer with a nudging coefficient of $3 \times 10^{-4} s^{-1}$.

Anthropogenic emissions of BC and other trace species in India and regions due east of India are taken from the Southeast Asia Composition, Clouds and Climate Coupling by Regional Study (SEAC^{4}RS) emissions inventory (Lu and Streets, 2012), while those in the regions due west of India and the shipping emissions are taken from MACCity emission inventory (Granier et al., 2011). The spatial distribution of anthropogenic BC emissions is shown in Figure 1 and shows highest values over the Indo-Gangetic Plain. The total annual anthropogenic BC emissions in this combined (SEAC^{4}RS+MACCity) emission inventory for South Asia (60^o-100^oE, 5^o-37^oN) are estimated as ~1195 Gg/year. These emission estimates are comparable to other regional inventories such as System for Air quality Forecasting And Research-India (SAFAR-India: ~1110 Gg/year) and Regional Emission Inventory for Asia (REAS: ~1170 Gg/year) but are significantly higher compared to Intercontinental chemical Transport Experiment Phase B inventory (INTEX-B: ~550 Gg/year). Note that SAFAR-India does not provide emissions outside India. Biomass burning emissions of trace gases and aerosols are obtained from the Fire Inventory from NCAR (Wiedinmyer et al., 2011) and are distributed in the model vertically following the online plume-rise module (Freitas et al., 2007). For the nearly two-month ICARB period (18 March–11 May 2006), total South Asian biomass burning emissions (327 Gg) of BC are higher than the total anthropogenic emissions (203 Gg) but ~80% of the biomass burning activity occurs in Burma (93^o-100^oE, 15^o-30^oN). Note that biomass burning represents emissions

only from open fires, while emissions from residential solid bio-fuel burning are included in the anthropogenic emissions. The parameterization used for other atmospheric processes along with schemes used for the biogenic and dust emissions are listed in Table 2.

This study implements 13 BC tracers in the WRF-Chem model to track BC emitted from different source types, sectors and regions. The tracer approach has been used previously in WRF-Chem to study the budget of CO in the USA (Pfister et al., 2011; Boynard et al., 2012) and South Asia (Kumar et al., 2013), but BC tracers are implemented for the first time in the model. BC tracers are artificial species added to the simulation and experience the same transport, physical, chemical and loss processes as a standard BC particle. However, the tracers do not affect the standard model results by modifying the radiation, atmospheric processes and aerosol properties.

We account for all sources of BC in the model by tracking BC emitted from anthropogenic (BC-ANT) and biomass burning (BC-BB) sources within the domain, and BC inflow from the lateral domain boundaries (BC-BDY). The BC-BDY tracer includes the contribution from all BC emission sources located outside the selected domain and therefore its distribution will provide information about background BC levels for South Asia. In addition, we track BC emitted from residential (BC-RES), transport (BC-TRA), industrial (BC-IND) and power-plants (BC-POW) sectors to estimate the contribution of different sectors to anthropogenic BC loadings. BC emissions from industrial, power and transportation sectors are mostly due to combustion of fossil fuels, while those from residential sectors are mostly due to biofuel combustion.

Five regional tracers track BC emitted from North, West, East and South India, and Burma (Figure 1). Anthropogenic emissions of BC from outside these five regions are also tracked separately and are classified as other regions. The initial and boundary conditions for all BC tracers are set to zero except boundary conditions for BC-BDY, which are set equal to BC from MOZART-4. The model simulations started on 15 Feb 2006 at 0000 UTC with a time step of 180 s, and model results are output every hour. The tracers are assumed to be well spun-up when the sum of BC tracers (BC_{trac}=BC-ANT+BC-BB+BC-BDY) approaches the total simulated BC. The time series of the relative difference between domain-wide averaged BC and BC_{trac} (Figure 2) at the first, 10^{th} and 20^{th} model level shows that the difference rapidly approaches 0% in the first 15 days of model run and remains close to zero for the rest of the model simulation. Thus, all tracers are spun up by 18 March 2006.

3 Model Evaluation

We first examine the ability of WRF-Chem in reproducing the variability and features of the BC distribution observed over the BoB and the AS during the ICARB campaign (Nair et al., 2008). The WRF-Chem predicted BC mass concentrations (surface layer) are bi-linearly interpolated to the ICARB ship track and compared to hourly ICARB BC measurements (Figure 3a). Both the model and observations show significantly higher BC levels in the BoB as compared to the AS. The average observed and modeled BC mass concentrations along the ship-track are estimated as 755±734 ng m^{-3} and 561±667 ng m^{-3}, respectively. The underestimation of BC by the chemical transport models has been a common problem in this region as has been shown in several previous studies (e.g. Nair et al., 2012; Moorthy et al., 2013). However, the ratio of measured to modeled value (1.3) in our study is closer to the lower end of the range (1.4-9) of the

corresponding ratios reported for marine sites in the Bay of Bengal and the Arabian Sea (Moorthy et al., 2013). The differences between WRF-Chem and observations could be related to the uncertainties in BC emission estimates, model transport and parameterization of aerosol processes. To evaluate the model's ability in capturing the spatial variability of BC observed along the ICARB ship-track, we compare co-located observed and WRF-Chem predicted latitudinal distribution of BC mass concentrations (Figure 4). Both the model and observed values are averaged over 1^{o} latitude bins for this comparison. The model successfully captures the latitudinal gradients of opposite sense in the BoB and AS with both the model and observations showing an increasing tendency in BC with latitude in the BoB but a decreasing tendency in the AS. The modeled values generally match within one standard deviation in the Bay of Bengal and in the southern part of the Arabian Sea, but are much lower north of 10^{o} N in the Arabian Sea.

The ICARB observations provide only a snapshot of the BC distribution because the ship was moving continuously in space and time (Figure 1). Here, we analyze the spatial distribution of BC mass concentrations averaged over the ICARB period (Figure 5a) to assess the representativeness of the ICARB ship-borne observations. As for the ship observations, the average modeled spatial distribution also shows more elevated BC levels in the BoB than the AS and latitudinal gradient of opposite sense in the BoB and the AS. This consistency of features deduced from ICARB observations with average model results indicates that ICARB ship-cruise was fairly well representative of the BoB and the AS during the pre-monsoon season.

In addition, we assess the model performance over the land by comparing WRF-Chem predicted BC values with average observed values reported for March to May at 12 stations in the model domain (Table 1). Average observed and modeled values at these sites range from 0.065 to 12 μg m^{-3} and 0.32-6.7 μg m^{-3}, respectively. Note that the differences between the model and observations in this study are much smaller than those found in previous studies. Moorthy et al. (2013) reported that the ratio of measured to modeled (GOCART and CHIMERE) at Delhi, Kharagpur, Trivandrum, Minicoy, Port-Blair and Nainital ranged between 0.7 to 6 while the corresponding ratios in our study vary from 0.7 to 2.6. Similarly, Nair et al. (2012) reported a ratio of 2 to 5 for different sites in India using the RegCM4 model. The largest difference between model and observations in our study was found at Lhasa (3.5), which could be related to the limited ability of the model in resolving the subgrid scale variations in the topography and location of emission sources (roadways, power plants, industries, residential burning etc.) at the resolution of 36 km^2. Seungkyu et al. (personal communication) showed that differences between the modeled and observed BC mass concentration in Kathmandu valley (an environment similar to Lhasa) can be reduced by a factor of about 4 if the emission sources are appropriately distributed according to their location as compared to the emissions averaged over grids of 5 km^2. The differences between our and previous studies could be related to use of both a different emission inventory and a different chemical transport model.

The results presented above demonstrate the model's ability to simulate the BC distribution in this region although with differences in the modeled and observed BC mass concentrations. The ability of the model to capture differences in the BC loadings over the BoB and the AS with better agreement between the model and observations compared to previous studies provides

confidence in using the model to understand why BC loading over the BoB is higher compared to the AS, and identifying the most important sources of BC in South Asia.

4 Results and Discussion

4.1 Differences in BC loading over the BoB and the AS

We first identify the sources affecting the ICARB ship-track by analyzing the time series of BC source tracers along the ship-track (Figure 3b) to gain insight into the differences in BC loading over the BoB and the AS. Model results suggest that anthropogenic emissions within the model domain were the main source of BC observed over both the BoB and the AS during ICARB. Biomass burning emission sources did not contribute more than 10% except during 5-8 April 2006, when the contribution of biomass burning exceeded 50%. The contribution of BC transported from the domain boundaries to the total BC mass concentration was less than 10% in the BoB but was up to 40% in the AS. The BC mass concentration due to anthropogenic (BC-ANT), biomass burning (BC-BB) and boundary (BC-BDY) sources along the ship track in the BoB are estimated to be 761±668, 113±129 and 33±5 ng m^{-3}, respectively, while the corresponding values in the AS are estimated to be 149±389, 7±6 and 22±12 ng m^{-3}, respectively. These numbers clearly show that higher BC loading in the BoB is a result of a much stronger influence of anthropogenic emission sources on the BoB compared to the AS. BC emitted from the biomass burning sources also make a significant contribution in the BoB but not in the AS.

To understand the differences in the influence of anthropogenic emissions over the BoB and the AS, we identify the regions where anthropogenic emission sources affecting the ICARB ship-track are located. Therefore, we analyze the contribution of anthropogenic sources located in

different regions of the domain to the total anthropogenic BC loading along the ICARB ship-track in the BoB and the AS (Table 3). The ICARB ship-track in the BoB was affected by all parts of India but the highest contribution is from East India (40%), which is the region of strongest BC emission in the domain (Figure 1). In contrast, the ICARB ship-track in the AS was affected mostly by South (~72%) India, where average anthropogenic BC emission rate is about 38% lower compared to East India.

To examine whether the results derived along the ICARB ship-track are true for the whole BoB and the AS, we analyze the contribution of different regional emission sources to anthropogenic BC loading in the whole BoB and the AS (last two rows of Table 3). For the whole BoB, we find source contributions very similar to what we found along the ship-track i.e. a significant contribution (>10%) from all parts of India with highest contribution from East India. In contrast, the source contributions over the whole AS deviate from what we found along the ICARB ship-track. South India remains the most important source region for the whole AS but the contribution reduces to 35% compared to 72% estimated along the ship-track. The contribution of West India (32%) is similar to South India for the whole AS and those of North India and other source regions are more than 10%. The above analysis shows that higher BC loading observed over the BoB compared to the AS during ICARB is a large-scale feature and results from a much stronger (about 5 times) influence of anthropogenic and biomass burning sources over the BoB.

4.2 Source contribution analysis for South Asia

To identify the most important sources of BC in South Asia, we analyze the spatial distributions of percentage contributions of anthropogenic (BC-ANT), biomass burning (BC-BB) and boundary inflow (BC-BDY) to total BC loadings in the model domain (Figures 5b-5d). Model results show large spatial variability in average total BC mass concentrations in South Asia with the highest values (>5000 ng m^{-3}) in the Indo-Gangetic Plain region, Mumbai-Pune region and Burma (93^{o}-100^{o}E, 15^{o}-30^{o}N). The BC-ANT distribution shows that anthropogenic emissions account for 60-95% of the total surface BC over India and in the cleaner regions of the Himalayas, the BoB and the AS. Elevated BC levels over Burma are mainly (>70%) due to biomass burning as evident from distribution of BC-BB. Biomass burning also contributes 20-50% of BC loadings in Nepal, eastern India and eastern BoB. The distribution of BC-BDY shows that emission sources located outside the domain contributes less than 5% to the BC loading over most parts of India, BoB and Burma, but makes a moderate contribution (up to 25%) in the AS and the Himalayas.

The spatial distributions of BC source tracers also help us to understand why latitudinal gradients of opposite sense were observed in the BoB and AS, and why BC showed an eastward increase due north of 13^{o}N in the BoB (Nair et al., 2008). The latitudinal gradients of the opposite sense were observed in the BoB and the AS because influence of anthropogenic emissions in the BoB decreased southwards while it increased southwards in the AS (Figure 5b). BC showed an eastward increase due north of 13^{o}N because eastern BoB was affected by both the anthropogenic and biomass burning sources while western BoB was affected mostly by the anthropogenic sources (Figures 5b and 5c).

The average mass concentrations of BC, BC-ANT, BC-BB and BC-BDY in South Asia (60^{o}-100^{o}E, 5^{o}-37^{o}N) during the ICARB period are given in Table 4. The contributions of BC-ANT, BC-BB and BC-BDY to the average total BC mass concentrations are estimated at about 60%, 37% and 3%, respectively. Large standard deviation of the average values reflects large spatial heterogeneity of BC mass concentrations.

While it is seen that anthropogenic emissions stand out as the major source of BC in the study domain in general, we identify the contribution of different sectors (such as residential (RES), industrial (IND), transportation (TRA), and power generation (POW)) to total anthropogenic BC loading (Figures 5e-5h). Among the different sectors, residential emissions account for more than 60% of the anthropogenic BC loading in Nepal, Bangladesh, Burma, Sri Lanka, Pakistan and Central India, while emissions from industrial sector dominate in some localized regions of North, West and East India. The dominance of residential biofuel burning sources is consistent with conclusions from previous studies in this region (e.g. Gustafsson et al., 2009). In the Himalayan regions, the transport sector (vehicular emissions) contributes 60-90% to the anthropogenic BC. BC emissions from shipping are included in the transport sector and thus we see higher contribution of transport sector in the AS compared to the BoB. The contribution of BC emissions from power plants is estimated to be less than 1% (not shown). The average mass concentrations of BC-RES, BC-IND, BC-TRA and BC-POW in South Asia (60^{o}-100^{o}E, 5^{o}-37^{o}N) during 18 March-11 May 2006 are given in Table 4. The emissions from residential, industrial, transport and power plant sectors contribute about 61%, 23%, 15% and 1%, respectively, to average BC-ANT mass concentrations. These contributions are very similar to the contributions of residential (62%), industrial (21%), transport (16%) and power plant (1%)

sectors to total anthropogenic emissions in South Asia indicating that surface BC mass concentrations are closely related to the emissions. However, we will show in the next section that such a close relation between surface BC concentrations and emissions does not exist in different regions of South Asia, because regional transport of BC makes an important contribution in different South Asian regions.

4.3 Local vs. regional anthropogenic sources

In this section, we examine whether surface BC mass concentration can also be related directly to the local BC emissions in different regions of South Asia as we saw for the whole South Asia in the previous section. To understand this, we first analyze the importance of regional transport by investigating the spatial distributions of surface BC emitted from anthropogenic sources located in North, West, East and South India, Burma and other regions averaged over 18 March-11 May 2006 at the surface (Figure 6). Anthropogenic sources in northern India contribute significantly (more than 100 ng m^{-3}) to the surface anthropogenic BC loadings in western and eastern parts of India, Burma and the BoB, and slightly influence parts of the AS along western Indian coastline. Northern Indian sources also contribute up to 50 ng m^{-3} in the Himalayan-Tibetan plateau region, but this contribution is smaller than that from other regions (50-200 ng m^{-3}). Analysis of diurnal variations of BC emitted from northern India and vertical wind component over the Tibetan region (81^{o}-90^{o}E, 30^{o}-35^{o}N) showed that transport of BC from North India to the Tibetan region likely occurs through upslope winds. However, more observations and fine scale modeling studies are required to lend further confidence in this process.

BC emitted by anthropogenic sources in western India contributes significantly to eastern and southern parts of India but the influence (>50 ng m^{-3}) also reaches to the BoB and parts of AS along western Indian coastline. Anthropogenic sources in eastern India significantly affect BC loadings in Burma, Bay of Bengal and South India but the influence does not reach the AS. South Indian anthropogenic sources affect both the BoB and the AS but the influence is higher in the BoB. Anthropogenic sources located in Burma do not make a significant impact in the BoB and the AS, while those located in other regions affect the southern parts of the BoB near Sri Lanka.

The contributions of BC emitted from different regions of South Asia to the total anthropogenic BC loadings in the five defined regions of South Asia, the AS and the BoB are summarized in Table 3. Here, we also quantify the contribution of local and regional sources to the anthropogenic BC loading in the different regions. The amount of BC due to sources located in a given region itself (e.g. BC-NI for northern India) is defined as a contribution from local sources, and BC coming from sources outside this region (e.g. BC-WI + BC-EI + BC-SI + BC-BR + BC-OT for northern India) is defined as contribution from the regional sources. The contribution of local sources is marked in bold font in Table 3. Local sources account for about 90% of the anthropogenic BC loading in North and South India, but regional sources contribute up to 30% in West and 21% in East India. Regional sources make a large contribution of 75% to the anthropogenic BC loading in Burma. However, it should also be noted that total anthropogenic BC loading in Burma is much smaller than the BC loading due to local biomass burning (Figure 5b-c).

The above analyses clearly highlight the importance of regional transport in controlling the distribution of BC over South Asia. To examine whether regional transport affects the relation between local emissions and surface BC mass concentrations, we compare the contributions of anthropogenic and biomass burning emissions to the total BC emissions as well as to the surface BC mass concentrations in different regions of South Asia. We estimate that anthropogenic emissions contribute about 90%, 90%, 45%, 75% and 3% to the total BC emissions in North, West, East and South India, and Burma respectively, while their contributions to surface BC mass concentrations are 93%, 95%, 69%, 90% and 18%, respectively. Similarly, the biomass burning emissions contribute about 10%, 10%, 55%, 25% and 97% of the total BC emission in North, West, East and South India, and Burma respectively, while the contributions of biomass burning emissions to the surface BC mass concentrations in these regions are 4%, 3%, 30%, 8% and 81% respectively. The sources located outside the model domain are the remaining contribution (less than 3%) in these regions. These results show that surface BC concentrations cannot be inferred directly from the emission inventories in different regions of South Asia.

We further examine the contributions of residential, industrial, transport and power generation sectors to total anthropogenic emissions as well as to the surface anthropogenic BC mass concentrations in North, West, East and South India, and Burma (Table 5). It is interesting to note that the contribution of BC emissions from different sectors to the total anthropogenic BC emissions as well as to the surface anthropogenic BC mass concentration are very similar in North, West, East and South India despite a significant contribution (up to 25%) of regional transport to surface total anthropogenic BC mass concentration in these regions (see Table 3). This is likely because of the fact that these geographical regions do not differ significantly in

terms of the relative contribution of different sectors to total anthropogenic BC emissions, and these relative contributions are maintained during transport of BC from one region to the other.

In contrast, Burma is different from the Indian regions as contributions of different sectors to total anthropogenic BC emissions and to the surface anthropogenic BC mass concentrations are not similar. The percent contributions of different sectors to the surface anthropogenic BC mass concentrations in Burma are more similar to the Indian regions, i.e. the highest contribution is from the residential sector followed by the industrial and transport sectors. This is likely because of the fact that regional transport of BC from the Indian regions is the main source (71%) of surface anthropogenic BC mass concentrations in Burma (see Table 5) and anthropogenic BC emissions in India are much stronger compared to Burma (see Figure 1). These results show that it is important to account for the contribution of regional transport while relating surface BC concentrations to emissions but the relationship between surface BC concentrations and local emissions may be preserved if emissions in the source region are weaker compared to the receptor region and relative contributions of different sectors to total emissions are similar in the source and receptor regions.

4. Summary

This study implemented source, sector and region specific BC tracers in the WRF-Chem model to understand the differences in BC loadings between the Bay of Bengal and the Arabian Sea, and assess the relative importance of different BC sources in South Asia during March-May 2006. The model reproduced the temporal and spatial variability of BC distribution observed during the ICARB ship-cruise. The average and standard deviation (representing the spatial and

453 temporal variability) in observed and modeled BC mass concentrations along the ship-track are
454 estimated as 755±734 ng m^{-3} and 561±667 ng m^{-3} respectively. Average modeled concentrations
455 at most of the inland stations were also found to fall within the range of observed values. The
456 model underestimates the observed BC mass concentrations but model observation discrepancy
457 in this study is found to be smaller compared to previous studies (Nair et al., 2012; Moorthy et
458 al., 2013).
459
460 Analysis of BC tracers shows that the ICARB ship-track in the BoB was affected by
461 anthropogenic sources located in all parts of India with highest contributions from East (40%)
462 and South (24%) India. In contrast, the AS was affected mostly by sources in South India. We
463 find that elevated levels of BC in the BoB were due to a much stronger anthropogenic influence
464 (5 times greater) in the BoB than the AS. Biomass burning in Burma also affects the BoB much
465 more strongly than the AS. The features of the BC distribution deduced from ICARB ship
466 observations were found to be consistent with model results averaged over larger spatial area and
467 time period (18 March-11 May 2006) indicating that ICARB measurements were fairly well
468 representative of the BoB and the AS during the pre-monsoon season.
469
470 Average modeled BC mass concentration in South Asia is estimated as 1341±2353 ng m^{-3} where
471 the high standard deviation reflects the large spatial and temporal variability. Analysis of BC
472 source tracers showed that anthropogenic emissions provided 60-95% of the total BC loading in
473 South Asia except in Burma where biomass burning played a major role during this period.
474 Biomass burning also contributed more than 20% to the BC in Nepal, eastern India and eastern
475 BoB. BC emissions from residential (61%) and industrial (23%) sectors are identified as major

anthropogenic sources in South Asia except in the Himalayas where vehicular emissions dominated. The transport emissions contribute up to 25% to surface BC mass concentrations in western and eastern India. We showed that it is important to account for the contribution of regional transport while relating surface BC concentrations to emissions in different regions of South Asia but the relationship between surface BC concentrations and local emissions may be preserved if emissions in the source region are weaker compared to the receptor region and/or relative contributions of different sectors to total emissions are similar in the source and receptor regions.

This study was conducted for March-May 2006 limiting our ability to extrapolate the results to other seasons or years. Kumar et al. (2015) simulated and analyzed BC seasonality for the year 2011. By comparing the March-May time period from the 2011 simulation with this current study, we can get an idea whether source attribution varies substantially between these two simulations. It should be noted that anthropogenic emissions in these two simulations are taken from two different emission inventories, SEAC^{4}RS + MACCity emissions, the 2006 (MACCity shipping emissions and emissions due west of India) to 2012 (SEAC^{4}RS emissions over rest of the domain) time period, for the 2006 simulation and EDGAR-HTAP emissions, which are appropriate for the 2010 time period, for the 2011 simulation. (The EDGAR-HTAP inventory was release after we conducted the 2006 simulation.) Therefore, differences in anthropogenic emissions between the simulations do not represent temporal changes in anthropogenic emissions appropriate for the two modeled years. However, the biomass burning emissions are based on the Fire Inventory from NCAR (FINN) in both the simulations and thus difference between the two simulations represents actual changes in the biomass burning emissions over

this region between 2006 and 2011. In comparing the emissions from the 2006 simulation to the 2011 simulation, the anthropogenic emissions changed from about 203 Gg to about 201 Gg, while the biomass burning emissions changed from about 327 Gg to 285 Gg for the ICARB period (18 March-11 May). The contribution of BC-ANT, BC-BB and BC-BDY to the total surface BC concentrations in the 2011 simulation are estimated as 65%, 28% and 7% respectively, while the corresponding contributions in the 2006 simulations are 60%, 37% and 3% respectively.

This comparison shows that changes in the strength of emission sources can potentially affect the source contribution analysis, but differences in meteorology between the two years can also play a role. Thus, multi-year simulations accounting for temporal variability in the strength of different emission sources and variability in meteorology must be conducted before these results can be applied to design BC mitigation strategies in South Asia. The effects of seasonal change in the strength of anthropogenic and biomass burning sources the source contribution analysis of BC in South Asia are discussed in a follow-up paper (Kumar et al., 2015). Nevertheless, this study illustrates the potential of integrating in situ observations with chemical transport modeling to understand processes controlling the distribution and variability of BC, and infer the most important sources of BC aerosol in a region.

Acknowledgments

We thank C. Knote for providing the basic WRF-Chem configuration used in this study. We thank F. Flocke, S. Madronich and C. Knote for their constructive comments on the manuscript. The datasets of initial and boundary conditions for meteorological fields is downloaded from http://dss.ucar.edu/datasets/ds083.2/data/. The datasets for initial and boundary conditions for chemical fields, biogenic emissions, biomass burning emissions and programs used to process these datasets are downloaded from the website http://www2.acd.ucar.edu/wrf-chem/. The National Center for Atmospheric Research is supported by the National Science Foundation. Authors acknowledge the ICARB project of ISRO-Geosphere Biosphere Program for providing the data collected onboard *Sagar Kanya*. We acknowledge ECCAD science team for providing emissions datasets. Comments from two anonymous reviewers are greatly appreciated.

Figures Captions

Figure 1: Spatial distribution of anthropogenic BC emissions over the model domain. Different regions from which BC emissions are tagged are shown with the Bay of Bengal and the Arabian Sea. Yellow line represents the ICARB ship-track, with the number standing for day of Month: Mr (March), Ap (April) and My (May). NI, WI, EI and SI represent North, West, East and South India, respectively.

Figure 2: Time series of percentage difference between total simulated BC and sum of all the BC tracers (BC_{trac}=BC-ANT+BC-BB+BC-BDY).

Figure 3: [a] WRF-Chem predicted and measured BC along the ICARB ship track during the ICARB period. [b] Percentage contributions of BC-ANT, BC-BB and BC-BDY to modeled BC.

Figure 4: WRF-Chem predicted and observed latitudinal gradients in BC mass concentrations along the ICARB ship-track in the Bay of Bengal and Arabian Sea regions. Horizontal bars represents one sigma (standard deviation) variation in BC mass concentration averaged over a 1^{o} latitude bin.

Figure 5: Spatial distributions of [a] total BC and [e] total anthropogenic BC mass concentration averaged over the ICARB period. Percentage contributions of BC-ANT [b], BC-BB [c], and BC-BDY to total BC, and BC-RES [f], BC-IND [g] and BC-TRA [h] to total anthropogenic BC.

Figure 6: Spatial distributions of anthropogenic BC emitted from North, West, East and South India, Burma, and other regions during the ICARB period. White solid lines mark the geographical boundaries of different regions.

Table Captions

Table 1: WRF-Chem simulated BC mass concentration (mean ± standard deviation) averaged over the period of 18 Mar to 11 May 2006, and observed range of average values during March – May at nine inland stations located in the model domain. The observed BC values are taken from the papers listed in the reference column.

Table 2: Parameterization used for selected atmospheric processes in WRF-Chem.

Table 3: Near surface mass concentration (ng m-3) of total anthropogenic BC (BC-ANT) and different anthropogenic regional BC tracers during the ICARB period along the ship-track in the AS and BoB, and over seven geogrpahical regions. Percentage contribution of each tracer to BC-ANT is also given in parenthesis. All numbers are rounded-off to the nearest whole number value. Numbers in bold font represent the contribution of local sources to the anthropogenic BC mass concentration of that region. BR and OT represent Burma and Other regions, respectively.

Table 4: : Average±standard deviation in mass concentration (ng m-3) of total BC, BC from anthropogenic sources (BC-ANT), from biomass burning (BC-BB), from model domain boundaries (BC-BDY), from residential (BC-RES), industrial (BC-IND), transportation (BC-TRA) and power generation (BC-POW) emissions averaged over South Asia (60^{o}-100^{o}E, 5^{o}-37^{o}N) during the ICARB period (March 18 – May 11). The standard deviation was calculated from all the BC values in South Asia and thus represents the spatial variability of modeled average BC values in South Asia.

Table 5: Percent contributions of residential (RES), industrial (IND), transport (TRA) and power generation (POW) sectors to the total anthropogenic emissions and to the surface anthropogenic BC mass concentrations in North (NI), West (WI), East (EI) and South India (SI), and Burma (BR).

References

Babu, S. S., Moorthy, K. K. and Satheesh, S. K.: Aerosol black carbon over Arabian Sea during inter monsoon and summer monsoon seasons, Geophys. Res. Lett., 31, L06104, doi:10.1029/2003GL018716, 2004.

Beegum, S. N., Moorthy, K. K., Babu, S. S., Satheesh, S. K., Vinoj, V., Badarinath, K. V. S., Safai, P. D., Devara, P. C. S., Singh, S., Vinod, Dumka, U. C., Pant, P.: Spatial distribution of aerosol black carbon over India during pre-monsoon season, Atmos. Environ., 43, 1071-1078, doi: 10.1016/j.atmosenv.2008.11.042, 2009.

Beljaars, A.C.M.: The parameterization of surface fluxes in large-scale models under free convection. Quart. J. Roy. Meteor. Soc., 121, 255–270, 1994.

Binkowski, F. S. and Shankar, U.: The regional particulate matter model: 1. Model description and preliminary results, J. Geophys. Res., 100, 26191-26209, doi: 10.1029/95JD02093, 1995.

Bollasina, M. A., Ming, Y., and Ramaswamy, V.: Earlier onset of the Indian monsoon in the late twentieth century: The role of anthropogenic aerosols, Geophys. Res. Lett., 40, 3715–3720, doi:10.1002/grl.50719, 2013.

Bonasoni, P., Laj, P., Marinoni, A., Sprenger, M., Angelini, F., Arduini, J., Bonafè, U., Calzolari, F., Colombo, T., Decesari, S., Di Biagio, C., di Sarra, A. G., Evangelisti, F., Duchi, R., Facchini, MC., Fuzzi, S., Gobbi, G. P., Maione, M., Panday, A., Roccato, F., Sellegri, K., Venzac, H., Verza, GP., Villani, P., Vuillermoz, E., and Cristofanelli, P.: Atmospheric Brown Clouds in the Himalayas: first two years of continuous observations at the Nepal Climate Observatory-Pyramid (5079 m), Atmos. Chem. Phys., 10, 7515-7531, doi:10.5194/acp-10-7515-2010, 2010.

Bond, T. C., Bhardwaj, E., Dong, R., Jogani, R. , Jung, S., Roden, C., Streets, D. G., and Trautmann, N. M.: Historical emissions of black and organic carbon aerosol from energy related combustion, 1850–2000, Global Biogeochem. Cy., 21, GB2018, doi:10.1029/2006GB002840, 2007.

Bond, T. C., Doherty, S. J., Fahey, D. W., Forster, P. M., Berntsen, T., DeAngelo, B. J., Flanner, M. G., Ghan, S., Kärcher, B., Koch, D., Kinne, S., Kondo, Y., Quinn, P. K., Sarofim, S., Schultz, M., Venkataraman, C., Zhang, H., Zhang, S., Bellouin, N., Guttikunda, S., Hopke, P. K., Jacobson, M. Z., Kaiser, J. W., Klimont, Z., Lohmann, U., Schwarz, J. P., Shindell, D., Storelvmo, T., Warren, S. G., and Zender, S.: Bounding the role of black carbon in the climate system: A scientific assessment, J. Geophys. Res.-Atmos., 118, 1–173, doi:10.1002/jgrd.50171, 2013.

Boynard, A., Pfister, G. G. and Edwards, D. P.: Boundary layer versus free tropospheric CO budget and variability over the United States during summertime, J. Geophys. Res., 117, D04306, doi:10.1029/20011JD016416, 2012.

Carrico, C. M., Bergin, M. H., Shrestha, A. B., Dibb, J. E., Gomes, L., Harris, J. M.: The importance of carbon and mineral dust to seasonal aerosol properties in the Nepal Himalayas, Atmos. Environ., 37, 2811-2824, doi: 10.1016/S1352-2310(03)00197-3, 2003.

Dockery, D. W., and Stone, P. H.: Cardiovascular risks from fine particulate air pollution, New England Journal of Medicine, 365, 511–513, 2007.

Easter, R. C., Ghan, S. J., Zhang, Y., Saylor, R. D., Chapman, E. G., Laulainen, N. S., Abdul-Razzak, H., Leung, L. R., Bian, X. and Zaveri, R. A.: MIRAGE: Model description and evalauation of aerosols and trace gases, J. Geophys. Res., 109, D20210, doi: 10.1029/2004JD004571, 2004.

617 Emmons, L. K., Walters, S., Hess, P. G., Lamarque, J.-F., Pfister, G. G., Fillmore, D., Granier,
618 C., Guenther, A., Kinnison, D., Laepple, T., Orlando, J., Tie, X., Tyndall, G., Wiedinmyer,
619 C., Baughcum, S. L., and Kloster, S.: Description and evaluation of the Model for Ozone and
620 Related chemical Tracers, version 4 (MOZART-4), Geosci. Model Dev., 3, 43-67,
621 doi:10.5194/gmd-3-43-2010, 2010.
622 Fast, J. D, Gustafson Jr.,W. I., Easter, R. C., Zaveri, R. A., Barnard, J. C., Chapman, E. G., and
623 Grell, G. A.: Evolution of ozone, particulates, and aerosol direct forcing in an urban area
624 using anew fully-coupled meteorology, chemistry, and aerosol model, J. Geophys. Res., 111,
625 D21305, doi: 10.1029/2005JD006721, 2006.
626 Freitas, S. R., Longo, K. M., Chatfield, R., Latham, D., Silva Dias, M. A. F., Andreae, M. O.,
627 Prins, E., Santos, J. C., Gielow, R., and Carvalho Jr., J. A.: Including the sub-grid scale
628 plume rise of vegetation fires in low resolution atmospheric transport models, Atmos. Chem.
629 Phys., 7, 3385-3398, doi:10.5194/acp-7-3385-2007, 2007.
630 Ginoux, P., Chin, M., Tegen, I., Prospero, J. M., Holben, B., Dubovik, O., and Lin, S. J.: Sources
631 and distributions of dust aerosols simulated with the GOCART model, J. Geophys. Res.-
632 Atmos., 106(D17), 20255–20273, 2001.
633 Granier, C. Bessagnet, B., Bond, T., D'Angiola, A., van der Gon, H. G., Frost, G. J., Heil, A.,
634 Kaiser, J. W., Kinne, S., Klimont, Z., Kloster, S., Lamarque, J.-F., Liousse, C., Masui, T.,
635 Meleux, F., Mieville, A., Ohara, T., Raut, J.-C., Riahi, K., Schultz, M. G., Smith, S. J.,
636 Thompson, A., van Aardenne, J., van der Werf, G. R. and van Vuuren, D. P.: Evolution of
637 anthropogenic and biomass burning emissions of air pollutants at global and regional scales
638 during the 1980–2010 period. , Climate Change 109 (1-2) : 163-190, doi: 10.1007/s10584-
639 011-0154-1, 2011.

Grell, G. A., Peckham, S. E., Schmitz, R., McKeen, S. A., Frost, G., Skamarock, W. C., and Eder, B.: Fully coupled "online" chemistry within the WRF model, Atmos. Environ., 39, 6957–6975, 2005.

Grell, G., and Devenyi, A. D.: A generalized approach to parameterizing convection combining ensemble and data assimilation techniques. Geophys. Res. Lett., 29, 1693, 2002.

Guenther, A., Karl, T., Harley, P., Wiedinmyer, C., Palmer, P. I., and Geron, C.: Estimates of global terrestrial isoprene emissions using MEGAN (Model of Emissions of Gases and Aerosols from Nature), Atmos. Chem. Phys., 6, 3181-3210, doi:10.5194/acp-6-3181-2006, 2006.

Gustafsson, O., Krusa, M., Zencak, Z., Sheesley, R. J., Granat, L., Engstrom, E., Praveen, P. S., Rao, P. S. P., Leck, C., and Rodhe, H.: Brown Clouds over South Asia: Biomass or Fossil Fuel Combustion?, Science, 323, 495–498, 2009.

Hodenbrog, Ø., Myhre, G., and Samset, H.: How shorter black carbon lifetime alters its climate effect, Nature Communications, 5, 5065, doi:10.1038/ncomms6065.

Hong, S.–Y., Noh, Y., and Dudhia, J: A new vertical diffusion package with an explicit treatment of entrainment processes. Mon. Wea. Rev., 134, 2318–2341, 2006.

Iacono, M. J., Delamere, J. S., Mlawer, E. J., Shephard, M. W., Clough, S. A., and Collins, W. D.: Radiative forcing by long–lived greenhouse gases: Calculations with the AER radiative transfer models. J. Geophys. Res., 113, D13103, 2008.

Knote, C., Hodzic, A., Jimenez, J. L., Volkamer, R., Orlando, J. J., Baidar, S., Brioude, J., Fast, J., Gentner, D. R., Goldstein, A. H., Hayes, P. L., Knighton, W. B., Oetjen, H., Setyan, A., Stark, H., Thalman, R., Tyndall, G., Washenfelder, R., Waxman, E., and Zhang, Q.:

Simulation of semi-explicit mechanisms of SOA formation from glyoxal in aerosol in a 3-D model, Atmos. Chem. Phys., 14, 6213-6239, doi:10.5194/acp-14-6213-2014, 2014.

Kumar, R., Barth, M. C., Madronich, S., Naja, M., Carmichael, G. R., Pfister, G. G., Knote, C., Brasseur, G. P., Ojha, N., and Sarangi, T.: Effects of dust aerosols on tropospheric chemistry during a typical pre-monsoon season dust storm in northern India, Atmos. Chem. Phys., 14, 6813-6834, doi:10.5194/acp-14-6813-2014, 2014b.

Kumar, R., Barth, M. C., Pfister, G. G., Nair, V. S., Ghude, S. D., and Ojha, N.: What controls the seasonality of cycle of BC in India?, J. Geophys. Res., submitted manuscript, 2015.

Kumar, R., Barth, M. C., Pfister, G. G., Naja, M., and Brasseur, G. P.: WRF-Chem simulations of a typical pre-monsoon dust storm in northern India: influences on aerosol optical properties and radiation budget, Atmos. Chem. Phys., 14, 2431-2446, doi:10.5194/acp-14-2431-2014, 2014a.

Kumar, R., Naja, M., Pfister, G. G., Barth, M. C., and Brasseur, G. P.: Simulations over South Asia using the Weather Research and Forecasting model with Chemistry (WRF-Chem): set-up and meteorological evaluation, Geosci. Model Dev., 5, 321-343, doi:10.5194/gmd-5-321-2012, 2012a.

Kumar, R., Naja, M., Pfister, G. G., Barth, M. C., and Brasseur, G. P.: Source attribution of carbon monoxide in India and surrounding regions during wintertime, J. Geophys. Res., 118, 1981-1995, doi:10.1002/jgrd.50134, 2013.

Kumar, R., Naja, M., Pfister, G. G., Barth, M. C., Wiedinmyer, C., and Brasseur, G. P.: Simulations over South Asia using the Weather Research and Forecasting model with Chemistry (WRF-Chem): chemistry evaluation and initial results, Geosci. Model Dev., 5, 619-648, doi:10.5194/gmd-5-619-2012, 2012b.

685 Lau, K. M., Kim, M. K. and Kim, K. M.: Asian summer monsoon anomalies induced by aerosol
686 direct forcing: The role of the Tibetan Plateau, Clim. Dyn., 26, 855–864,
687 doi:10.1007/s00382-006-0114-z, 2006.
688 Lawrence, M. G. and Lelieveld, J.: Atmospheric pollutants outflow from southern Asia: a
689 review, Atmos. Chem. Phys., 10, 11017-11096, doi:10.5194/acp-10-11017-2010, 2010.
690 Lu, Z., and Streets, D. G.: The Southeast Asia Composition, Cloud, Climate Coupling Regional
691 Study Emission Inventory, http://bio.cgrer.uiowa.edu/SEAC4RS/emission.html, last access:
692 24 Aug 2014, 2012.
693 Lu, Z., Zhang, Q., and Streets, D. G.: Sulfur dioxide and primary carbonaceous aerosol
694 emissions in China and India, 1996–2010, Atmos. Chem. Phys., 11, 9839-9864,
695 doi:10.5194/acp-11-9839-2011, 2011
696 Marrapu, P., Cheng, Y., Beig, G., Sahu, S., Srinivas, R., and Carmichael, G. R.: Air quality in
697 Delhi during the CommonWealth Games, Atmos. Chem. Phys. Discuss., 14, 10025-10059,
698 doi:10.5194/acpd-14-10025-2014, 2014.
699 Menon, S., Koch, D., Beig, G., Sahu, S., Fasullo, J., and Orlikowski, D.: Black carbon aerosols
700 and the third polar ice cap, Atmos. Chem. Phys., 10, 4559–4571, doi:10.5194/acp-10-4559-
701 2010, 2010.
702 Moorthy, K. K., Beegum, S. N., Srivastava, N., Satheesh, S. K., Chin, M., Bond, N., Babu, S. S.,
703 and Singh, S.: Performance evaluation of chemistry transport models over India,
704 Atmospheric Environment, 71, 210-225, doi:10.1016/j.atmosenv.2013.01.056, 2013.
705 Moorthy, K. K., Satheesh, S. K. and Babu, S. S.: Integrated Campaign for Aerosols, Gases and
706 Radiation Budget (ICARB): An overview, J. Earth Sys. Sci., 117, S1, 243-262, 2008.

Morrison, H., Thompson, G., and Tatarskii, V.: Impact of Cloud Microphysics on the Development of Trailing Stratiform Precipitation in a Simulated Squall Line: Comparison of One– and Two–Moment Schemes. Mon. Wea. Rev., **137,** 991–1007, 2009.

Nair, V. S., Babu, S. S., and Moorthy, K. K.: Aerosol characteristics in the marine atmospheric boundary layer over the Bay of Bengal and Arabian Sea during ICARB: Spatial distribution and latitudinal gradients, J. Geophys. Res., 113, D15208, doi:10.1029/2008JD009823, 2008.

Nair, V. S., Babu, S. S., Moorthy, K. K., Sharma, A. K., and Ajai, A. M.: Black carbon aerosols over the Himalayas: direct and surface albedo forcing, Tellus B, 65, 19738, http://dx.doi.org/10.3402/tellusb.v65i0.19738, 2013.

Nair, V. S., Solmon, F., Giorgi, F., Mariotti, L., Babu, S. S., and Moorthy, K., K.: Simulation of South Asian aerosols for regional climate studies, J. Geophys. Res., 117, D04209, doi:10.1029/2011JD016711, 2012.

Neu, J. L. and Prather, M. J.: Toward a more physical representation of precipitation scavenging in global chemistry models: cloud overlap and ice physics and their impact on tropospheric ozone, Atmos. Chem. Phys., 12, 3289-3310, doi:10.5194/acp-12-3289-2012, 2012.

Pathak, B., Kalita, G., Bhuyan, K., Bhuyan, P. K., and Moorthy, K. K.: Aerosol temporal characteristics and its impact on shortwave radiative forcing at a location in the northeast of India, J. Geophys. Res.-Atmos., 115, D19204, doi:10.1029/2009jd013462, 2010.

Pfister, G. G., Avise, J., Wiedinmyer, C., Edwards, D. P., Emmons, L. K., Diskin, G. D., Podolske, J., and Wisthaler, A.: CO source contribution analysis for California during ARCTAS-CARB, Atmos. Chem. Phys., 11, 7515-7532, doi:10.5194/acp-11-7515-2011, 2011.

729 Pöschl, U.: Atmospheric aerosols: composition, transformation, climate and health effects,
730 Angew. Chem. Int. Ed., 2005, 44, 7520-7540, 2005.
731 Ram, K., Sarin, M. M., and Tripathi, S. N.: A 1 year record of carbonaceous aerosols from an
732 urban site in the Indo-Gangetic Plain: Characterization, sources and temporal variability, J.
733 Geophys. Res.- Atmos., 115, D24313, doi:10.1029/2010jd014188, 2010.
734 Ramanathan, V., and Carmichael, G.: Global and regional climate changes due to black carbon,
735 Nature Geosci., 1, 221-227, 2008.
736 Ramanathan, V., Chung, C., Kim, D., Bettge, T., Buja, L., Kiehl, J. T., Washington, W. M., Fu,
737 Q., Sikka, D. R., and Wild, M.: Atmospheric Brown Clouds: Impacts on South Asian Climate
738 and Hydrological Cycle, Proc. Natl. Acad. Sci. USA, 102(15), 5326–5333, 2005.
739 Reddy, M. S., Boucher, O., Balkanski, Y., and Schulz, M.: Aerosol optical depths and direct
740 radiative perturbations by species and source types, Geophys. Res. Lett., 32, L12803, doi:
741 10.1029/2004GL021743, 2005.
742 Satheesh, S. K., and Ramanathan, V.: Large differences in tropical aerosol forcing at the top of
743 the atmosphere and Earth's surface, Nature, 405, 60-62, 2000.
744 Skamarock, W. C., Klemp, J. B., Dudhia, J., Gill, D. O., Barker, D. M., Wang, W., and Powers,
745 J. G.: A description of the advancedresearch WRF version 2, NCAR Tech. Note, NCAR/TN-
746 468+STR, Natl. Cent. for Atmos. Res., Boulder, Colo, availableat: http://wrf-
747 model.org/wrfadmin/publications.php, last access: 24 Aug 2014, 2008.
748 Srivastava, S., Lal, S., Venkataramani, S., Gupta, S., and Sheel, V.: Surface distributions of O3,
749 CO and hydrocarbons over the Bay of Bengal and the Arabian Sea during pre-monsoon
750 season, Atmos. Environ., 47, 459-467, 2012.

751 Tewari, M., Chen, F., Wang, W., Dudhia, J., LeMone, M. A., Mitchell, K., Ek, M., Gayno, G.,
752 Wegiel, J., and Cuenca, R. H.: Implementation and verification of the unified NOAH
753 land surface model in the WRF model. 20th conference on weather analysis and
754 forecasting/16th conference on numerical weather prediction, pp. 11–15, 2004.
755 Tie, X., Madronich, S.,Walters, S., Edwards, D. P., Ginoux, P., Mahowald, N., Zhang, R., Lou,
756 C., and Brasseur, G.: Assessment of the global impact of aerosols on tropospheric oxidants, J.
757 Geophys. Res., 110, D03204, doi:10.1029/2004JD005359, 2005.
758 Unger, N., Bond, T. C., Wang, J. S., Koch, D. M., Menon, S., Shindell, D. T., and Bauer, S.:
759 Attribution of climate forcing to economic sectors, Proc. Natl. Acad. Sci., 107, 3382-3387,
760 doi:10.1073/pnas.0906548107, 2010.
761 Unger, N., Shindell, D. T., and Wang, S.: Climate forcing by the on-road transportation and
762 power generation sectors, Atmos. Environ., 43, 3077-3085,
763 doi:10.1016/j.atmosenv.2009.03.021, 2009.
764 Verma, S., Venkataraman, C., and Boucher, O.: Attribution of aerosol radiative forcing over
765 India during the winter monsoon to emissions from source categories and geographical
766 regions, Atmos. Environ., 45, 4398-4407, 2011.
767 Wang, Q., Jacob, D. J., Spackman, J. R., Perring, A. E., Schwarz, J. P., Moteki, N., Marais, E.
768 A., Ge, C., Wang, J., and Barrett, S. R. H.: Global budget and radiative forcing of black
769 carbon aerosol: Constraints from pole-to-pole (HIPPO) observations across the Pacific, J.
770 Geophys. Res. Atmos., 119, 195–206, doi:10.1002/2013JD020824, 2014.
771 Wesely, M. L.: Parameterization of surface resistance to gaseous dry deposition in regional-scale
772 numerical models, Atmos. Environ., 23, 1293–1304, doi:10.1016/0004-6981(89)90153-4,
773 1989.

774 Wiedinmyer, C., Akagi, S. K., Yokelson, R. J., Emmons, L. K., Al-Saadi, J. A., Orlando, J. J.,
775 and Soja, A. J.: The Fire INventory from NCAR (FINN): a high resolution global model to
776 estimate the emissions from open burning, Geosci. Model Dev., 4, 625-641,
777 doi:10.5194/gmd-4-625-2011, 2011.
778 Yasunari, T. J., Bonasoni, P., Laj, P., Fujita, K., Vuillermoz, E., Marinoni, A., Cristofanelli, P.,
779 Duchi, R., Tartari, G., and Lau, K.-M.: Estimated impact of black carbon deposition during
780 pre-monsoon season from Nepal Climate Observatory – Pyramid data and snow albedo
781 changes over Himalayan glaciers, Atmos. Chem. Phys., 10, 6603-6615, doi:10.5194/acp-10-
782 6603-2010, 2010.
783 Zaveri, R., Easter, R., Fast, J. and Peters, L.: Model for simulating aerosol interactions and
784 chemistry (MOSAIC), J. Geophys. Res., 113, D13204, doi:10.1029/2007JD008782, 2008.
785 Zhang, X., Y., Wang, Y. Q., Zhang, X. C., Guo, W., and Gong, S. L.: Carbonaceous aerosol
786 composition over various regions of China during 2006, J. Geophys. Res.-Atmos., 113,
787 D14111, doi:10.1029/2007jd009525, 2008.

Table 1: WRF-Chem simulated BC mass concentration (mean ± standard deviation) averaged over the period of 18 Mar to 11 May 2006, and observed range of average values during March – May at nine inland stations located in the model domain. The observed BC values are taken from the papers listed in the reference column.

Site Name	(Lat, Lon, Alt)	Mean Observed range (March-May)	WRF-Chem (18Mar – 11 May 2006)	References
Delhi	(28.6^{o}N, 77.2^{o}E, 260 m)	8-12 μg m^{-3}	6.7 ± 4.0 μg m^{-3}	Beegum et al., (2009)
Kanpur	(26.4^{o}N, 80.3^{o}E, 142 m)	2-5 μg m^{-3}	4.7 ± 2.7 μg m^{-3}	Ram et al., (2010)
Kharagpur	(22.5^{o}N, 87.5^{o}E, 28 m)	2-5 μg m^{-3}	3.7 ± 2.8 μg m^{-3}	Beegum et al., (2009)
Dibrugarh	(27.3^{o}N, 94.6^{o}E, 111m)	5-10 μg m^{-3}	3.7 ± 3.1 μg m^{-3}	Pathak et al., (2010)
Trivandrum	(8.5^{o}N, 76.9^{o}E, 3m)	1.8-3 μg m^{-3}	0.9±0.6 μg m^{-3}	Beegum et al., (2009)
Minicoy	(8.3^{o}N, 73.0^{o}E, 1m)	0.065-0.22 μg m^{-3}	0.24±0.15 μg m^{-3}	Beegum et al., (2009)
Port-Blair	(11.6^{o}N, 92.7^{o}E, 60m)	1.3-1.8 μg m^{-3}	0.7±0.8 μg m^{-3}	Beegum et al., (2009)
Nainital	(29.4^{o}N,79.5^{o}E,1958 m)	0.8-1.5 μg m^{-3}	1.2 ± 0.8 μg m^{-3}	Beegum et al., (2009)
Nagarkot	(27.7^{o}N,85.5^{o}E,2150 m)	1.5 μg m^{-3}	1.3 ± 1.1 μg m^{-3}	Carrico et al., (2003)
Lhasa	(29.7^{o}N, 91.1^{o}E, 3663 m)	2-3 μg m^{-3}	0.42 ± 0.25 μg m^{-3}	Zhang et al., (2008)
Langtang	(28.1^{o}N,85.6^{o}E,3920 m)	0.5 μg m^{-3}	0.8 ± 0.5 μg m^{-3}	Carrico et al., (2003)
NCO-P	(28.0^{o}N,86.8^{o}E,5079 m)	0.2-0.4 μg m^{-3}	0.46 ± 0.39 μg m^{-3}	Bonasoni et al., (2010)

792 **Table 2:** Parameterization used for selected atmospheric processes in WRF-Chem.

Process	Parameterization
Cloud microphysics	Morrison double moment (Morrison et al., 2009)
Radiation	RRTMG short- and long-wave (Iacono et al., 2008)
Surface layer	MM5 similarity scheme (Beljaars, 1994)
Land surface model	Noah land surface (Tewari et al., 2004)
Planetary boundary layer	Yonsei university scheme (Hong et al., 2006)
Cumulus parameterization	Grell-3D (Grell and Devenyi, 2002)
Gas-phase chemistry	MOZART (Emmons et al., 2010; Knote et al., 2014)
Photolysis	Fast Troposphere Ultraviolet Visible (Tie et al., 2005)
Dry deposition	Wesely (Wesely, 1989)
Wet deposition	Neu and Prather (Neu and Prather, 2012)
Biogenic emissions	MEGAN (Guenther et al., 2006)
Dust emissions	GOCART (Ginoux et al., 2001)

793

Table 3: Near surface mass concentration (ng m^{-3}) of total anthropogenic BC (BC-ANT) and different anthropogenic regional BC tracers during the ICARB period along the ship-track in the AS and BoB, and over seven geogrpahical regions. Percentage contribution of each tracer to BC-ANT is also given in parenthesis. All numbers are rounded-off to the nearest whole number value. Numbers in bold font represent the contribution of local sources to the anthropogenic BC mass concentration of that region. BR and OT represent Burma and Other regions, respectively.

Region	BC-ANT[a]	BC-NI[a]	BC-WI[a]	BC-EI[a]	BC-SI[a]	BC-BR[a]	BC-OT[a]
Along the ICARB ship-track							
AS	149±389	7±6 (4%)	20±18 (14%)	4±3 (3%)	107±377 (72%)	-	10±9 (7%)
BoB	761±668	159±148 (21%)	98±61 (13%)	305±410 (40%)	182±23 (24%)	1±1 (-)	18±21 (3%)
Geographical Regions							
North India	1245±612	**1145±592 (92%)**	22±18 (2%)	54±48 (4%)	5±6 (-)	-	20±5 (2%)
West India	1679±863	256±191 (15%)	**1261±706 (75%)**	89±81 (5%)	50±37 (3%)	-	22±7 (1%)
East India	2411±898	262±120 (11%)	99±40 (4%)	**1853±868 (77%)**	148±75 (6%)	31±18 (1%)	19±6 (1)
South India	1657±678	75±57 (5%)	195±98 (12%)	80±100 (5%)	**1282±580 (77%)**	-	25±7 (1%)
Burma	945±224	142±66 (15%)	76±31 (8%)	328±123 (35%)	97±40 (10%)	**276±121 (29%)**	26±20 (3%)
AS	102±62	12±13 (11%)	33±40 (32%)	3±3 (2%)	36±22 (35%)	-	18±9 (18%)
BoB	563±508	112±102 (20%)	74±36 (13%)	234±369 (42%)	114±58 (20%)	9±16 (2%)	19±6 (3%)

[a]Mean±Sigma (standard deviation)

Table 4: Average±standard deviation in mass concentration (ng m-3) of total BC, BC from anthropogenic sources (BC-ANT), from biomass burning (BC-BB), from model domain boundaries (BC-BDY), from residential (BC-RES), industrial (BC-IND), transportation (BC-TRA) and power generation (BC-POW) emissions averaged over South Asia (60^{o}-100^{o}E, 5^{o}-37^{o}N) during the ICARB period (March 18 – May 11). The standard deviation was calculated from all the BC values in South Asia and thus represents the spatial variability of modeled average BC values in South Asia.

Total BC	BC-ANT	BC-BB	BC-BDY	BC-RES	BC-IND	BC-TRA	BC-POW
1341±2353	810±1179	497±1919	34±6	497±687	187±629	120±134	5±11

Table 5: Percent contributions of residential (RES), industrial (IND), transport (TRA) and power generation (POW) sectors to the total anthropogenic emissions and to the surface anthropogenic BC mass concentrations in North (NI), West (WI), East (EI) and South India (SI), and Burma (BR).

Region	Percent contribution to anthropogenic BC emissions				Percent contribution to surface anthropogenic BC mass concentration			
	RES	IND	TRA	POW	RES	IND	TRA	POW
NI	62	23	14	1	62	22	15	1
WI	56	33	11	1	55	33	12	1
EI	70	19	10	1	68	20	11	1
SI	64	23	12	1	61	26	12	1
BR	79	3	18	1	69	17	14	1

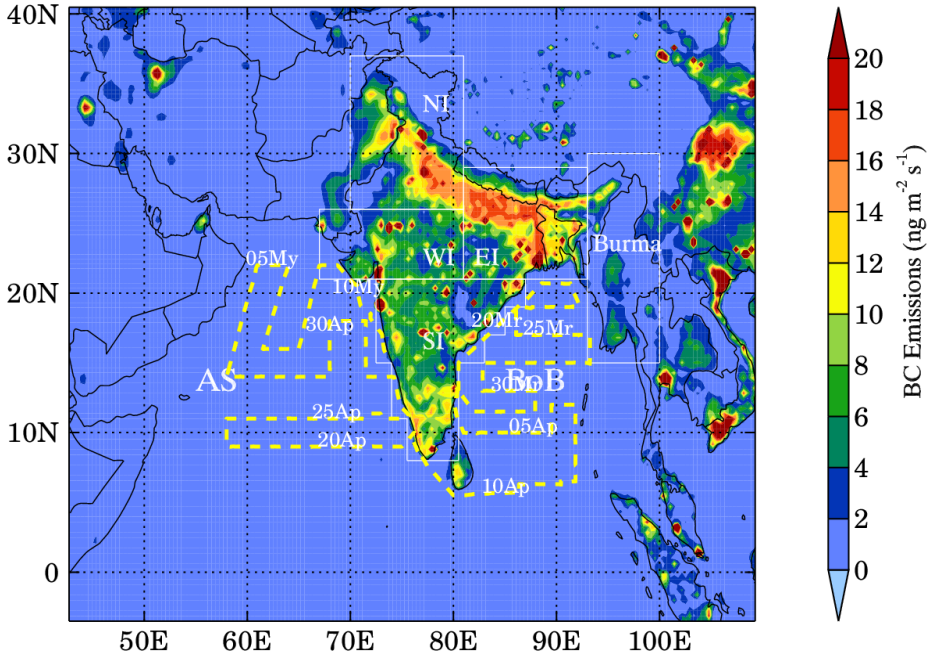

Figure 1: Spatial distribution of anthropogenic BC emissions over the model domain. Different regions from which BC emissions are tagged are shown with the Bay of Bengal and the Arabian Sea. Yellow line represents the ICARB ship-track, with the number standing for day of Month: Mr (March), Ap (April) and My (May). NI, WI, EI and SI represent North, West, East and South India, respectively.

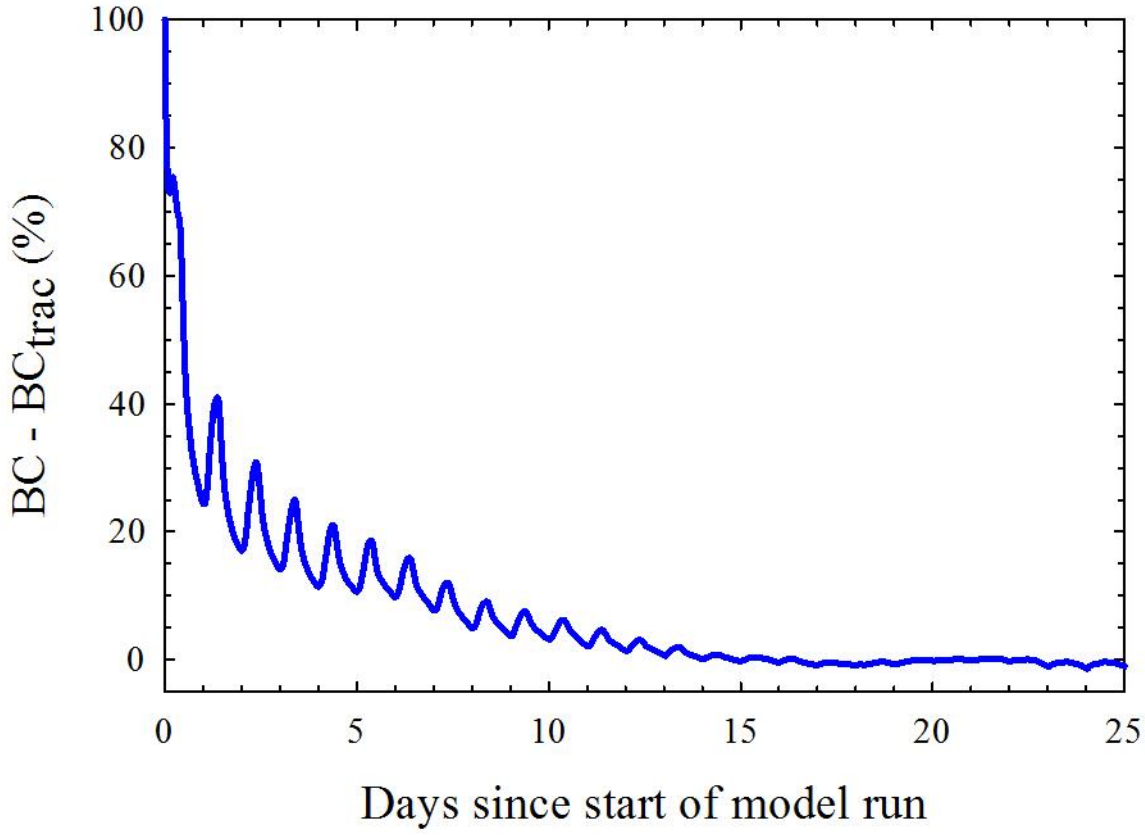

821

822 **Figure 2:** Time series of percentage difference between total simulated BC and sum of all the

823 BC tracers (BC_{trac}=BC-ANT+BC-BB+BC-BDY).

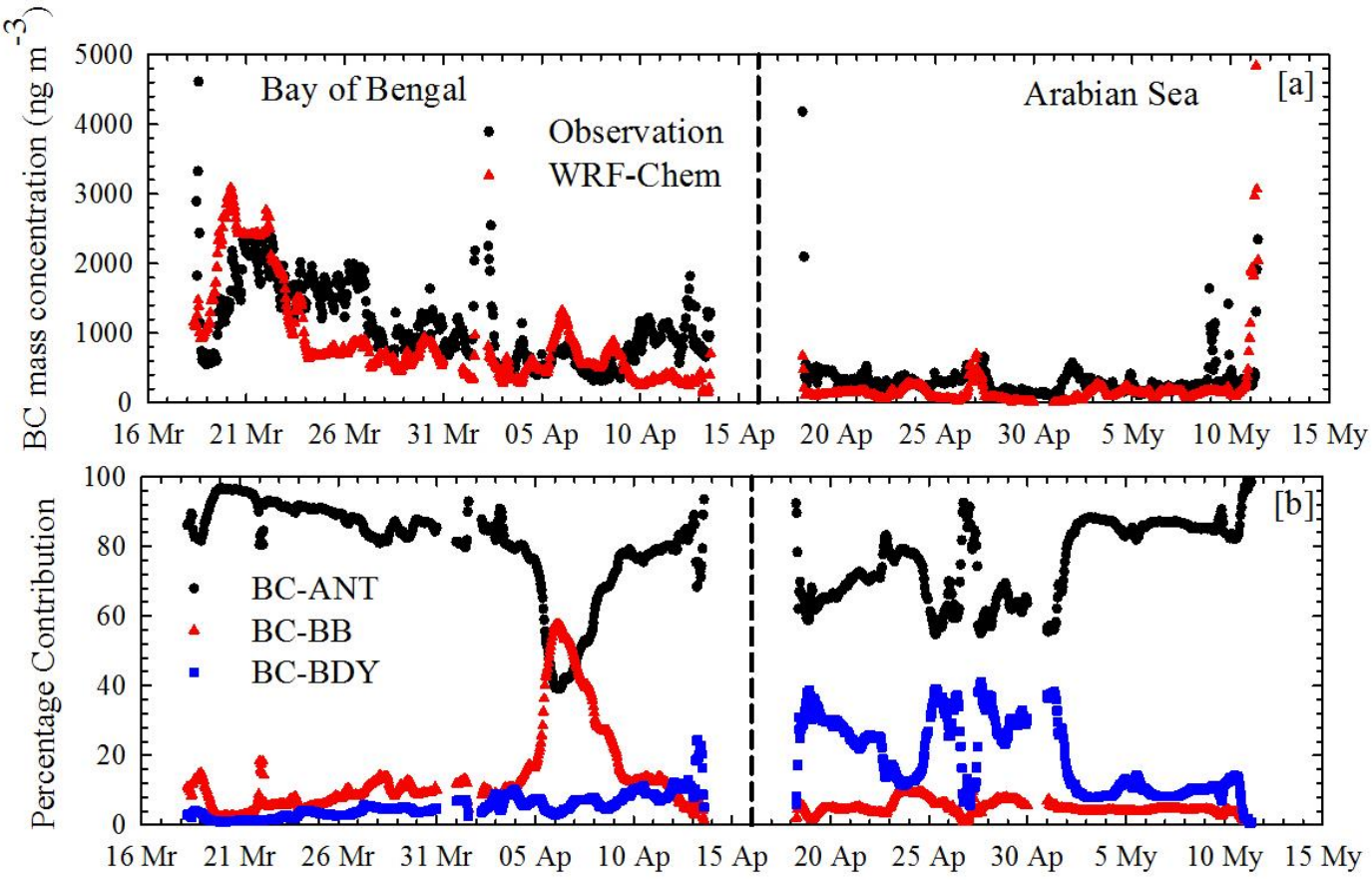

824
825 **Figure 3:** [a] WRF-Chem predicted and measured BC along the ICARB ship track during the

826 ICARB period. [b] Percentage contributions of BC-ANT, BC-BB and BC-BDY to modeled BC.

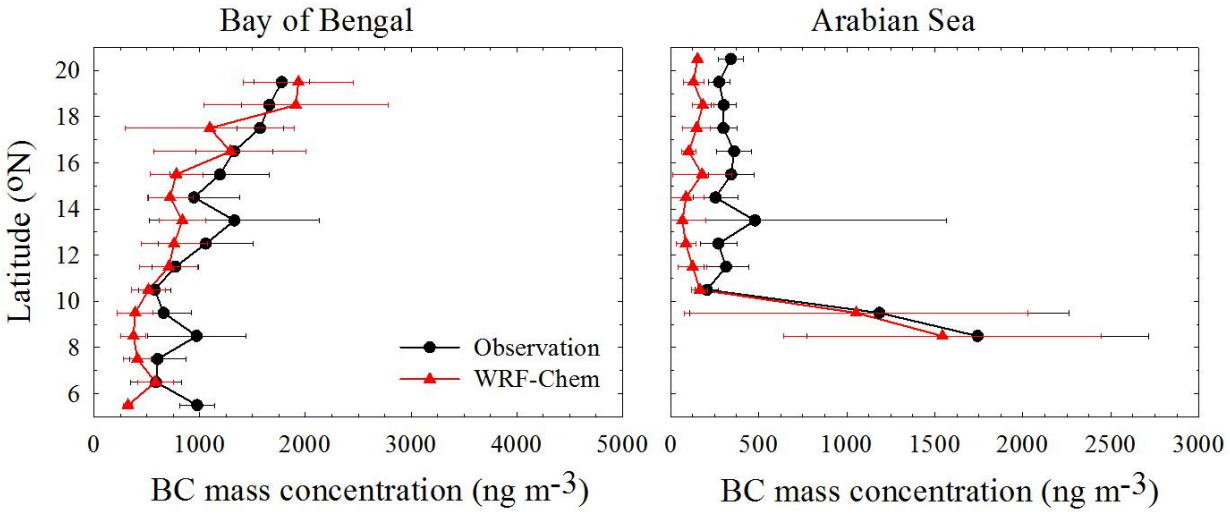

827

828 **Figure 4**: WRF-Chem predicted and observed latitudinal gradients in BC mass concentrations
829 along the ICARB ship-track in the Bay of Bengal and Arabian Sea regions. Horizontal bars
830 represents one sigma (standard deviation) variation in BC mass concentration averaged over a 1^{o}
831 latitude bin.

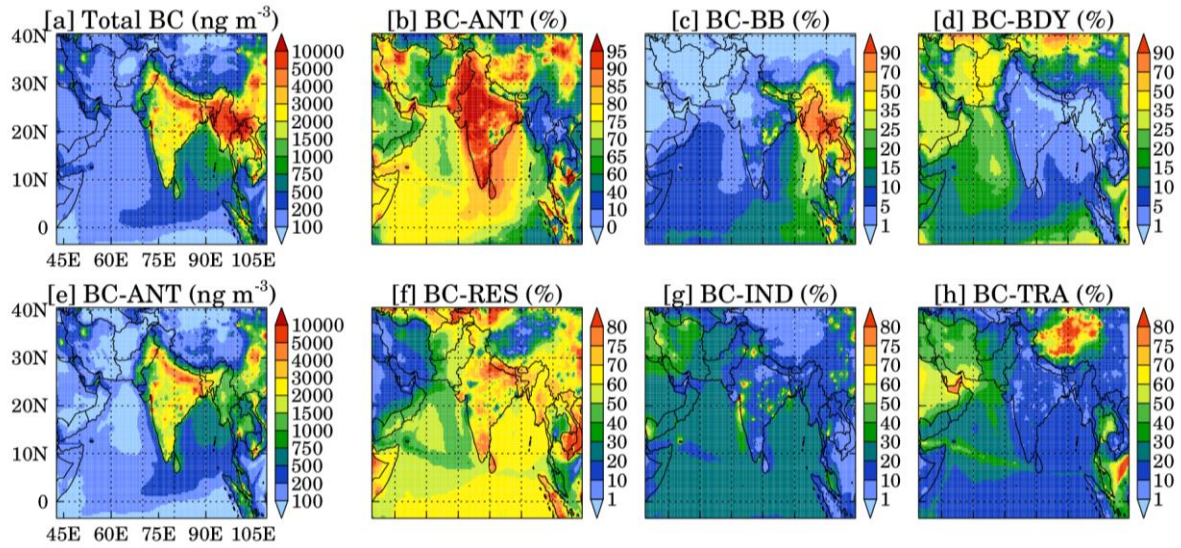

832

833 **Figure 5:** Spatial distributions of [a] total BC and [e] total anthropogenic BC mass concentration

834 averaged over the ICARB period. Percentage contributions of BC-ANT [b], BC-BB [c], and BC-

835 BDY to total BC, and BC-RES [f], BC-IND [g] and BC-TRA [h] to total anthropogenic BC.

836

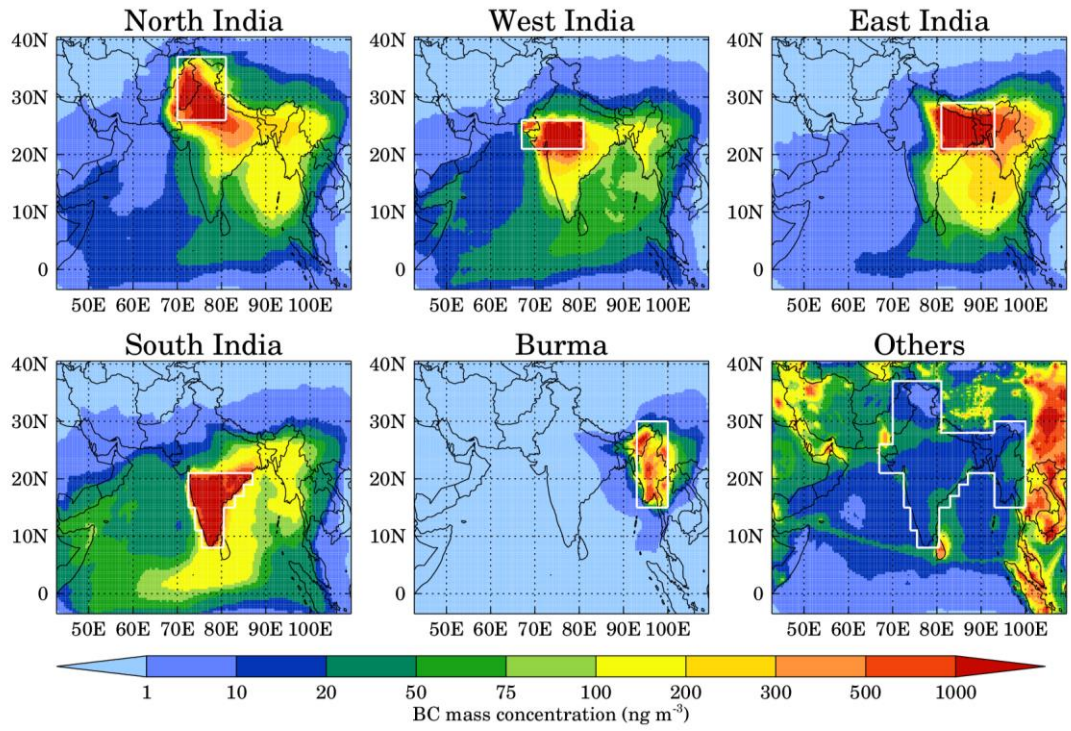

Figure 6: Spatial distributions of anthropogenic BC emitted from North, West, East and South India, Burma, and other regions during the ICARB period. White solid lines mark the geographical boundaries of different regions.